

# Peptide-amphiphile nanofibers: A versatile scaffold for the preparation of self-assembling materials

Jeffrey D. Hartgerink, Elia Beniash, and Samuel I. Stupp\*

Departments of Chemistry and Materials Science and Engineering and the Medical School, Northwestern University, Evanston, IL 60208

Edited by Jack Halpern, University of Chicago, Chicago, IL, and approved February 12, 2002 (received for review December 26, 2001)

**Twelve derivatives of peptide-amphiphile molecules, designed to self-assemble into nanofibers, are described. The scope of amino acid selection and alkyl tail modification in the peptide-amphiphile molecules are investigated, yielding nanofibers varying in morphology, surface chemistry, and potential bioactivity. The results demonstrate the chemically versatile nature of this supramolecular system and its high potential for manufacturing nanomaterials. In addition, three different modes of self-assembly resulting in nanofibers are described, including pH control, divalent ion induction, and concentration.**

Preprogrammed noncovalent bonds, within and between molecules, build highly functional and dynamic structures in biology, which motivates our interest in self-assembly of synthetic systems. Over the past few decades a substantial amount of literature describing noncovalent self-assembly of nanostructures has accumulated (1–14). However, it is still difficult to design supramolecular structures, particularly if we want to start with designed molecules and form objects that measure between nanoscopic and macroscopic dimensions. Developing this ability will take us closer to the broad, bottom-up approach of self-assembly observed in biology.

Our laboratory has studied over the past decade self-assembly of designed molecules into macromolecular structures of two-dimensional (15, 16), one-dimensional (17, 18), and zero-dimensional nature (19–22). These self-assembled objects contain between  $10^1$  and  $10^5$  molecules and thus resemble synthetic and biological polymers in molar mass. The interactions that lead to the formation of these structures include chiral dipole–dipole interactions,  $\pi$ – $\pi$  stacking, hydrogen bonds, nonspecific van der Waals interactions, hydrophobic forces, electrostatic interactions, and repulsive steric forces. All systems studied involved combinations of these forces that counterbalance the enormous translational and rotational entropic cost caused by polymolecular aggregation. In some cases the possibility of internally linking these self-assembled structures through covalent bonds has been explored (1, 17, 20, 23). A cross-linking produces actual polymers whose various shapes and dimensionalities are controlled by self-assembly and are very different from the well-known “beads-on-a-chain” structures of traditional polymers.

In our studies of self-assembling systems we also have explored self-organization at length scales much greater than those of the aggregates themselves, reaching into scales of microns, millimeters, and even centimeters. We also have been interested in functionalities that emerge from self-assembly at these larger-length scales. An interesting example was the layering and polar stacking of mushroom-shaped supramolecular structures each measuring about 5 nm. The stem-to-cap layers of these nanostructures result in centimeter-scale films that are spontaneously piezoelectric (24). The search for useful systems in the microscopic and macroscopic regime that take advantage of molecular self-assembly probably will require a combination of top-down and bottom-up approaches such as ours.

Very recently we have explored the self-assembly of peptide amphiphiles (PA) in water into one-dimensional cylindrical objects, nanometers in diameter but microns in length (17). These molecules are interesting because they can be used to

inscribe biological signals in the self-assembled structure. In this system, PA 4 (Fig. 1) was chosen for the self-assembling building block to combine the advantages of peptides with those of amphiphiles that are known to self-assemble into sheets, spheres, rods, disks, or channels depending on the shape, charge, and environment (25). Amphiphiles with a conical shape in which the hydrophilic head group is somewhat bulkier than its narrow hydrophobic tail have been shown to form cylindrical micelles. Examples include single-chain lipids with ionic head groups such as SDS and hexadecyltrimethylammonium bromide (26). Depending on the composition, amphiphilic peptides have been shown to organize peptide secondary structure and aggregation state (27–30). PAs synthesized previously with mono- or di-alkyl tails were found to associate in conformations such as triple helical structures found in collagen (31–38). Modification of this strategy allowed us to design a cone-shaped, ionic amphiphile that could assemble into cylindrical micelles or peptide nanofibers (17). Because of the ionic nature of the head group, self-assembly could be induced reversibly by changing the pH of the PA solution.

To enhance the physical and chemical robustness of these supramolecular fibers, an intermolecular crosslinking scheme using four consecutive cysteine residues was included in our design. Upon oxidation of the self-assembled fibers intermolecular disulfide bonds are formed that stitch the fiber into a high molecular weight fibrous polymer. Because this crosslinking scheme uses disulfide bonds this also allows the crosslinking to be self-correcting and reversible as is often seen in natural protein folding and disulfide bond formation (39). Because the surface chemistry of the fiber can be controlled by modifying the C-terminal region of the peptide, it is also a good scaffold to nucleate crystals or adsorb molecules in a specific orientation. In this regard our initial work on this subject demonstrated nucleation of hydroxyapatite nanocrystals with c-axis orientation along the fiber axis, which mimics the geometrical relationship between apatite crystals and collagen fibrils in bone (40, 41).

In this work we demonstrate the structural versatility of the PA self-assembly into nanofibers. By modifying the alkyl tail length and peptide amino acid composition we examine the role played by different structural units in these designed molecules. Furthermore we also describe here three different methods to induce self-assembly, thereby further expanding its versatility.

## Materials and Methods

**Chemicals.** Except as noted below, all chemicals were purchased from Fisher or Aldrich and used as provided. Diisopropylethylamine and piperidine were redistilled before use. Amino acid derivatives, derivatized resins, and 2-(1h-benzotriazole-1-yl)-1,1,3,3-tetramethyluronium hexafluorophosphate were purchased from Nova Biochem. All water used was deionized with a Millipore Milli-Q water purifier operating at a resistance of 18 M $\Omega$ .

This paper was submitted directly (Track II) to the PNAS office.

Abbreviations: PA, peptide-amphiphile; TEM, transmission electron microscopy.

\*To whom reprint requests should be addressed. E-mail: s-stupp@northwestern.edu.

CHEMISTRY

SPECIAL FEATURE

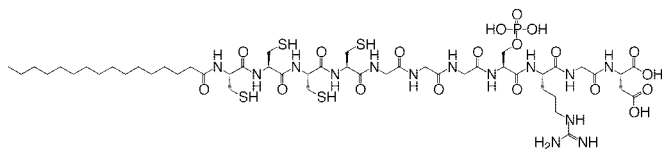


Fig. 1. Chemical structure of PA 4.

**Synthesis of the PAs.** The PAs were prepared on a 0.25-mmol scale by using standard fluorenylmethoxycarbonyl chemistry on an Applied Biosystems 733A automated peptide synthesizer. All peptides prepared have a C-terminal carboxylic acid and were made by using prederivatized Wang resin with the exception of peptide 10. In the case of peptide 10, 1 equivalent of Wang resin was reacted with three equivalents of fluorenylmethoxycarbonyl-Ser(PO<sub>3</sub>Bnzl)-OH, four equivalents of 1-(mesitylene-2-sulfonyl)-3-nitro-1H-1,2,4-triazole, and six equivalents of 1-methylimidazole in dichloromethane. After the peptide portion of the molecule was prepared, the resin was removed from the automated synthesizer and the N terminus was capped with a fatty acid containing 6, 10, 16 or 22 carbon atoms. The alkylation reaction was accomplished by using two equivalents of the fatty acid, two equivalents 2-(1h-benzotriazole-1-yl)-1,1,3,3-tetramethyluronium hexafluorophosphate, and six equivalents of diisopropylethylamine in dimethylformamide. The reaction was allowed to proceed for at least 6 h after which the reaction was monitored by ninhydrin. The alkylation reaction was repeated until the ninhydrin test was negative. In general the longer the fatty acid the more repetitions were required to drive the reaction to completion.

Cleavage and deprotection of the PAs containing cysteine was done with a mixture of trifluoroacetic acid, water, triisopropyl silane, and ethanedithiol in a ratio of 91:3:3:3 for 3 h at room temperature. The cleavage mixture and two subsequent trifluoroacetic acid washings were filtered into a round-bottom flask. The solution was roto-evaporated to a thick viscous solution. This solution was triturated with cold diethylether. The white precipitation was collected by filtration, washed with copious cold ether, and dried under vacuum. Typically, 200 mg of the PA powder was dissolved in 20 ml of water with the addition of 1 M NaOH to adjust the pH of the solution to 8 and 200 mg of DTT to reduce all cysteine amino acids to the free thiol and allowed to stir overnight. The solution was then filtered through a 0.2- $\mu$ m nylon Acros filter into a new round-bottom flask. This 10 mg/ml (1% by weight) solution was used for all subsequent manipulations. Work-up of PAs not containing cysteine were performed as above except that ethanedithiol was omitted from the cleavage reaction and DTT was not used in the preparation of aqueous solutions. PAs were characterized by

Table 1. List of PA molecules

Molecule	N terminus	Peptide (N to C)	Charge pH 7
1	H	CCCCGGGS <sup>(PO<sub>4</sub>)</sup> RGD	-2
2	C <sub>6</sub> H <sub>11</sub> O	CCCCGGGS <sup>(PO<sub>4</sub>)</sup> RGD	-3
3	C <sub>10</sub> H <sub>19</sub> O	CCCCGGGS <sup>(PO<sub>4</sub>)</sup> RGD	-3
4	C <sub>16</sub> H <sub>31</sub> O	CCCCGGGS <sup>(PO<sub>4</sub>)</sup> RGD	-3
5	C <sub>22</sub> H <sub>43</sub> O	CCCCGGGS <sup>(PO<sub>4</sub>)</sup> RGD	-3
6	C <sub>10</sub> H <sub>19</sub> O	AAAAGGGGS <sup>(PO<sub>4</sub>)</sup> RGD	-3
7	C <sub>16</sub> H <sub>31</sub> O	AAAAGGGGS <sup>(PO<sub>4</sub>)</sup> RGD	-3
8	C <sub>16</sub> H <sub>31</sub> O	CCCCGGGS <sup>(PO<sub>4</sub>)</sup>	-3
9	C <sub>16</sub> H <sub>31</sub> O	CCCCGGGS <sup>(PO<sub>4</sub>)</sup> KGE	-3
10	C <sub>16</sub> H <sub>31</sub> O	CCCCGGGS <sup>(PO<sub>4</sub>)</sup> RGDS	-3
11	C <sub>16</sub> H <sub>31</sub> O	CCCCGGGSRGD	-1
12	C <sub>16</sub> H <sub>31</sub> O	CCCCGGGEIKVAV	-1

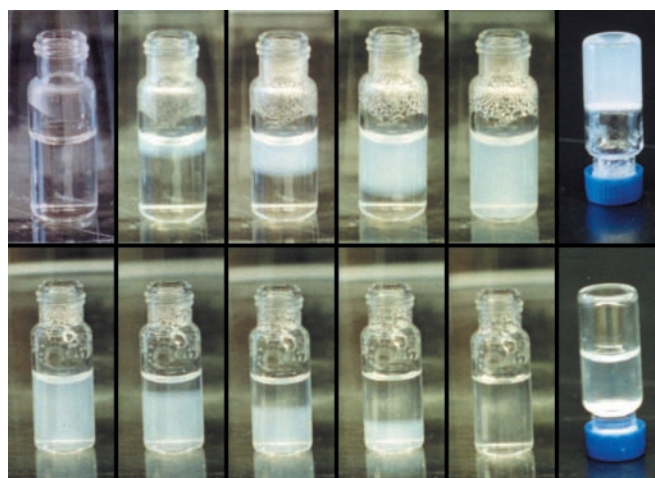


Fig. 2. Time sequence of pH-controlled PA self-assembly and disassembly. (Upper) From left to right molecule 6 dissolved in water at a concentration of 0.5% by weight at pH 8 is exposed to HCl vapor. As the acid diffused into the solution a gel phase is formed, which self-supports upon inversion (Far Left). (Lower) The same gel is treated with NH<sub>4</sub>OH vapor, which increases the pH and disassembles the gel, returning it to a fully dissolved solution.

matrix-assisted laser desorption ionization–time of flight MS and were found to have the expected molecular weight.

**Acid-Induced Self-Assembly.** Samples of the PA in question were prepared as above and placed in a small glass vial with an open top. This vial and a second vial filled with 12 M HCl were placed together in a sealed glass chamber where the HCl vapor was allowed to slowly diffuse into the PA solution.

**Divalent Ion-Induced Self-Assembly.** One hundred microliters of 10 mg/ml solution of PA 4 was treated with 1 M CaCl<sub>2</sub> (adjusted to pH 6) drop-wise in 1- $\mu$ l increments. The solutions were shaken after each addition of the CaCl<sub>2</sub> solution to obtain better diffusion of the metal ions.

**Covalent Capture of the Assembled Fiber.** The gels formed above were treated with 0.05 M I<sub>2</sub>, which was adjusted to a pH of 3.5.

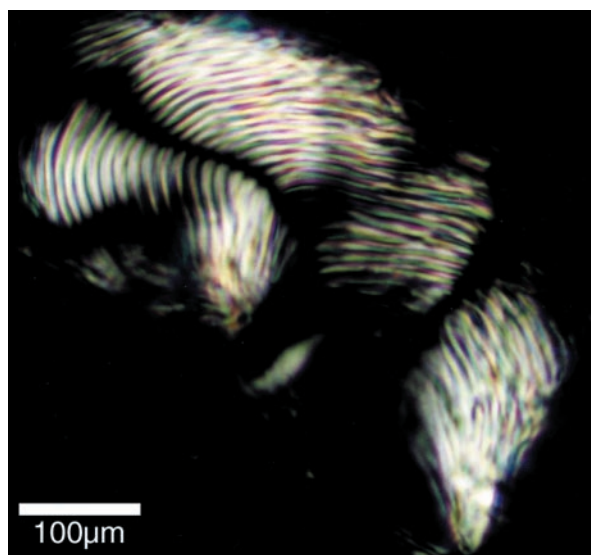


Fig. 3. Light microscopy image of a gel formed from PA 4 between crossed polarizers. Birefringence indicates orientation of the material at the level of tens of microns.

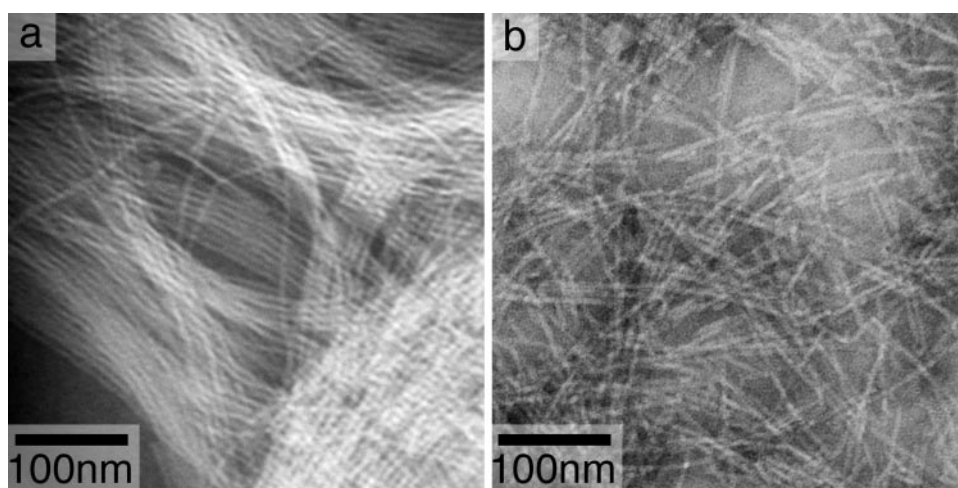


Fig. 4. TEM image of fibers formed from molecules **3** (a) and **5** (b). Samples were negatively stained with phosphotungstic acid.

The iodine solution was placed on top of the gel and allowed to slowly diffuse into the gel. After the iodine color had completely penetrated the gel, excess iodine was removed. The gel was then soaked in a bath of deionized water, which was periodically changed until the discoloration from the iodine was gone as judged by eye (roughly 48 h depending on the size of the gel). The formation of the disulfide bonds was monitored by Fourier transform-IR (Fig. 9, which is published as supporting information on the PNAS web site, [www.pnas.org](http://www.pnas.org)). After oxidation the spectra revealed the effective disappearance of the S-H stretching peak at  $2,556\text{ cm}^{-1}$ .

**Transmission Electron Microscopy (TEM).** Samples of the PAs were prepared in two different ways. In some cases a small sample of the gel, prepared in bulk as described above, was smeared onto a holey carbon-coated TEM grid (Quantifoil, Jena, Germany). Other samples were prepared directly on the grid by placing  $10\ \mu\text{l}$  of 0.01–0.02% solution of PA directly on the grid. The grid was then placed into a sealed chamber with HCl vapors for 10 min after which the grids were washed with deionized water. Two routine staining techniques, negative staining with phosphotungstic acid or positive staining with uranyl acetate, were used in this study (42). In all cases electron microscopy was performed at an accelerating voltage of 200 kV.

## Results and Discussion

In an attempt to gain a better understanding of which components of the PA motif are responsible for its self-assembly properties and to explore the extent to which the molecule can tolerate modifications for use in other applications, 12 derivatives of the PA were prepared as shown in Table 1. In particular, three regions of the molecule were modified. First, the alkyl tail, which provides the hydrophobic driving force for self-assembly, was varied from as long as a 22-carbon fatty acid to molecules containing no fatty acid at all. Second, the tetra-cysteine region was replaced by a tetra-alanine repeat to determine the effects of the thiol groups on self-assembly. Finally, the head group region of the molecule (the C-terminal end), which is the segment of the molecule that interacts with the environment, was modified to incorporate different cell adhesion ligands and crystal nucleation centers.

**Effect of Hydrophobic Tail Length on Self-Assembly.** Five different molecules with the peptide sequence  $\text{CCCCGGGS}^{(\text{PO}_4)}\text{RGD}$  (molecules **1–5**) were prepared and dissolved in water at a concentration between 10% and 0.001% by weight at pH 8. Upon

acidification it was found that molecules **3–5** formed a precipitate even at a concentrations as low as 0.001% by weight (0.01 mg/ml). Molecule **2** precipitated only at concentrations above 1% by weight whereas molecule **1** was pH-insensitive. When a solution of molecules **3, 4, or 5** was slowly acidified above a concentration of 0.25% by weight the solution forms a self-supporting gel (Fig. 2). The micrograph in Fig. 3 shows the optical texture of the gel at high concentration (12% by weight), revealing striations on the order of 10 microns wide, which are reminiscent of a cholesteric liquid crystalline phase. If molecules **3–5** were not fully reduced with DTT before acidification or were intentionally oxidized with  $\text{I}_2$ , subsequent acidification did not produce a gel. Instead the PA was found to precipitate as an off-white powder. Examination of the precipitate by polarized light microscopy revealed that it was not birefringent. Negative-stain TEM showed no particular supramolecular structure but rather irregular clumps with a wide size distribution. In contrast, the material precipitated from fully reduced solutions of molecules **3–5** when investigated by negative-stain TEM were found to form a dense network of fibers in excess of  $1\ \mu\text{m}$  long and 5–8

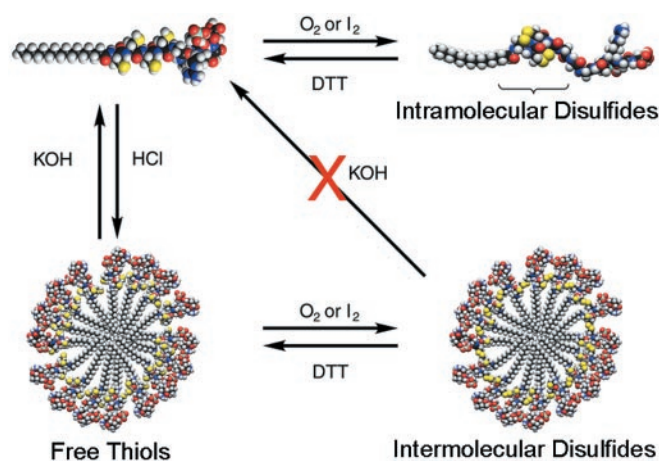
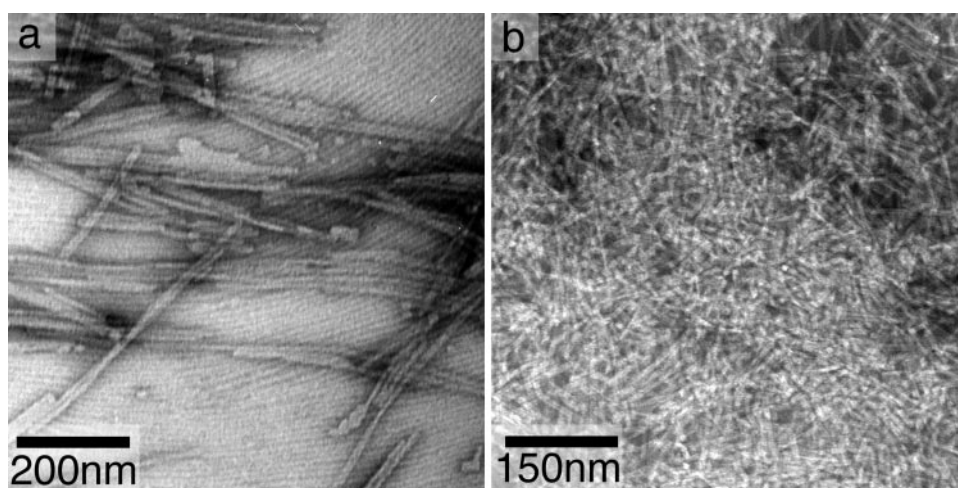


Fig. 5. Schematic illustrating the self-assembly and covalent capture of the PAs based on pH and oxidation state. Molecules self-assemble upon acidification and disassemble at neutral and basic pH when fully reduced. Molecules that are oxidized will not self-assemble at acidic pH, likely because of the distorted conformation required by intramolecular disulfide bonds. Supramolecular fibers that are oxidized (polymerized) lose their sensitivity to pH and are thus stable across a much broader range of pH, including physiological.



**Fig. 6.** TEM image of fibers formed from molecules **6** (a) and **7** (b). Samples were negatively stained with phosphotungstic acid. PA **6** displays a strong tendency to form parallel arrays of fibers whereas PA **7** does not.

nm in diameter (Fig. 4). In contrast, the precipitate formed by molecule **2** formed only aggregates of random size and shape.

The pH sensitivity of the different PAs can be explained as follows. When the pH of the solution is near neutrality the peptides have a net negative charge, which keeps PA molecules from self-assembly as a result of electrostatic repulsion. Upon acidification this negative charge is eliminated and hydrophobic tails can now begin to aggregate. The pH insensitivity observed in PA **1**, a molecule without an alkyl tail, is a clear indication that the hydrophobic effect (43) plays a key role in self-assembly in water. Although PA **2** has a hydrophobic tail, it is apparently not long enough to favor thermodynamically the extensive formation of nanofiber networks. This could be the result of geometrical effects as described by Israelachvili *et al.* (44) or to a weaker hydrophobic effect. However, the system is sensitive to pH, suggesting a different aggregation mechanism occurs in water after electrostatic repulsive forces are decreased. In contrast, PAs **3–5** have sufficiently long hydrophobic tails to make the cylindrical packing the most favorable. However, if PAs **3–5** are partially oxidized, formation of intramolecular disulfide bonds prevents the formation of nanofibers. This observation suggests that conformational changes introduced by intramolecular disulfide bonds suppress self-assembly.

Interestingly, formation and structure of the nanofibers pre-

pared from this PA was found to be unaffected by the starting concentration. However, a second level of organization, that was concentration-dependent, was revealed by TEM images. This involved the formation of flat parallel bundles containing many nanofibers. As the concentration of PA was increased the percentage of fibers involved in bundle formation increased. Given that three-dimensional networks of the high aspect ratio objects must form for gelation to occur (45), this observation would naturally explain why gelation occurs only beyond a certain threshold PA concentration of  $\approx 0.25\%$  by weight.

In our previous work we showed that self-assembled nanofibers formed by molecule **4** can be covalently captured by the formation of disulfide bonds upon oxidation with iodine (17). The same procedure was found to work for molecules **3** and **5**. Fig. 5 summarizes schematically the reversibility of both self-assembly and covalent capture in these systems. Other peptide systems have been previously reported that exhibit pH-reversible gelation (46); however, our system adds versatility to this self-assembly scaffold because of its reversible polymerization.

**Elimination of Crosslinking Function.** We also examined here the effect of the PA crosslinking region on self-assembling behavior. Although the cysteine residues can lead to reversible covalent capture of the nanofibers, there are some applications in which

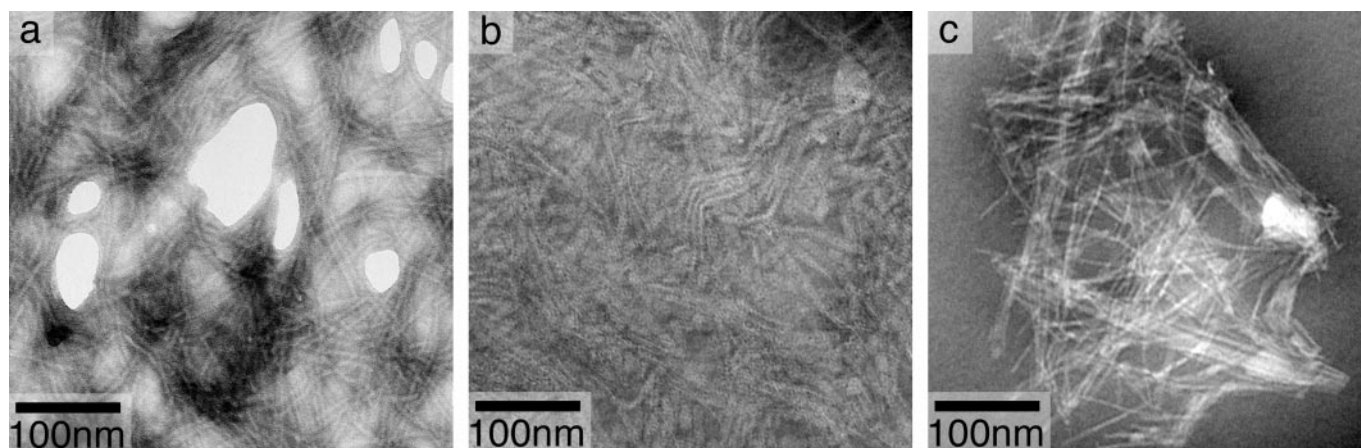


**Fig. 7.** TEM images of fibers formed from molecules **9** (a), **11** (b), and **12** (c). Samples were negatively stained with phosphotungstic acid. Although fibers with a diameter between 5 and 8 nm are formed in all cases, the length and stiffness of the fibers formed vary considerably.

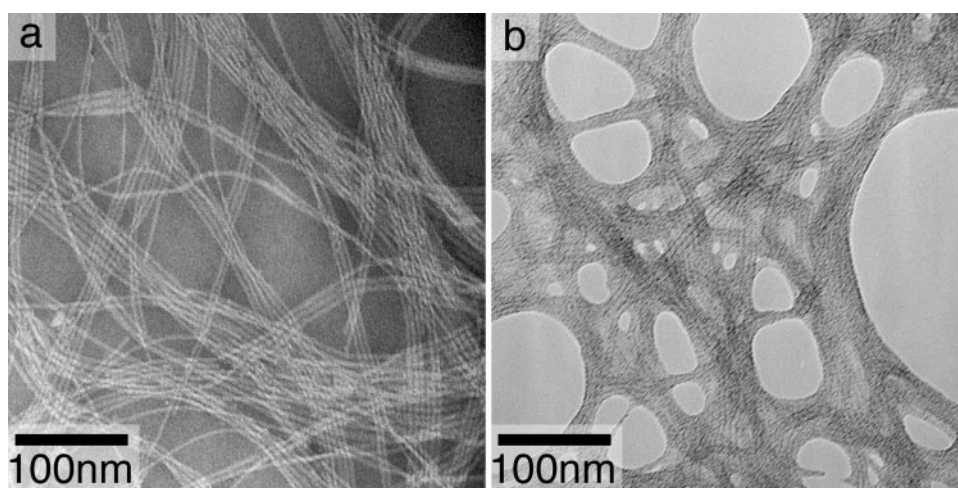


**Fig. 8.** TEM images of molecule **3** (a) self-assembled by drying directly onto a TEM grid without adjusted pH and molecule **4** (b) self-assembled by mixing with  $\text{CaCl}_2$ . Molecule **3** is negatively stained with phosphotungstic acid whereas molecule **4** is positively stained with uranyl acetate. In both cases the same fibrous morphology is observed as is seen by pH-induced self-assembly.

the presence of thiols can be problematic, such as catalysis. For example, transition metal catalysts can be poisoned by sulfur (47). Furthermore, the cysteines must be fully reduced for self-assembly to be successful, which requires that this be done in the presence of DTT or in an anaerobic environment. To eliminate this problem, the cysteine amino acids were replaced by alanine. Two derivatives were prepared, one with a C10 alkyl tail (molecule **6**) and one with a C16 alkyl tail (molecule **7**). Self-assembly was accomplished by gas-phase acidification as before and in both cases a self-supporting gel was formed at concentrations of 0.2% and above. Examination of the gels by negative-stain TEM revealed that the gels are made up of nanofibers with similar structure compared with the cysteine-containing nanofibers. This finding indicates the presence of cysteine residues is not required for self-assembly. However, in the case of molecule **6** the propensity for packing into broad ribbons of fibers appears to be much higher (Fig. 6a). In contrast, molecule **7**, although maintaining the same fiber superstructure, appears to form almost no parallel arrangements between fibers (Fig. 6b). Additionally, this gel when examined after several days exhibits some degree of phase separation. Even though it is not clear at this point why this occurs, it may well be an indication of a transition from a kinetic gel to a more thermodynamically stable state.

**Versatility of the Hydrophilic C-Terminal Region.** The third region of the PA investigated for modification is the head group of the molecule, which is exposed on the surface of nanofibers after self-assembly. It is this portion of the molecule that will interact directly with the environment and may be modified to enhance bioactivity, control mineralization of inorganic structures, promote catalysis, or gain other desirable properties. PAs **8–12** were prepared to establish whether this region could be altered while still maintaining a fibrous morphology. Molecules **8–10** and **12** were prepared to examine the ability to display chemistries with different cell adhesion properties. In the original design of the PAs we included phosphoserine to control mineralization (17). In this work we synthesized derivatives **11** and **12** to determine whether phosphorylation is required for self-assembly. In one case, molecule **12**, we used the sequence IKVAV because of its known role as a cell adhesion ligand in laminin (48, 49). This molecule differs from the original PA, which contains the integrin binding sequence RGD, because it has significant hydrophobic content and also

lacks a phosphate group. PA **8**, which does not contain a bioactive sequence, was also found to form nanofibers. At the same time, PAs **9** and **10**, which contain control sequences for bioactivity experiments, were also found to exhibit self-assembling behavior. Interestingly, despite chemical differences, the general design of our self-assembling scaffold is conducive to the formation of one-dimensional nanostructures (Fig. 7). However, our TEM observations show that fibers differ in length and stiffness. For example PA **6** fibers are longer than PA **7** (Fig. 6), whereas fibers formed by PA **12** appear to be stiffer than ones formed by PA **11**.

**Different Modes of Self-Assembly.** Finally, we also explored alternative modes of promoting self-assembly that do not require pH changes. These alternative modes may be of interest for the use of these systems in medicine. The pH-triggered mechanism we used is a powerful method to control the state of aggregation, but it also restricts the noncrosslinked supramolecular structures to particular pH regimes. First, we found that self-assembly can occur by simply taking a PA dissolved in water at pH 8 and placing it on a surface that is allowed to dry (for example, directly on a carbon-coated TEM grid). Upon examination of this preparation by negative-stain TEM we clearly observed the formation of nanofibers (Fig. 8a). We are not sure at the moment what the mechanism is that drives self-assembly at this high pH; however, three important factors are likely to be charge screening by the surface and increased concentration of salts and PA as the water evaporates. We have also found that treatment of a solution of PA **4** with a divalent ion, such as  $\text{Ca}^{2+}$ , immediately causes gelation of the solution. In contrast, treatment of PA samples with  $\text{K}^+$  up to 6 M does not lead to gelation or self-assembly. When examined by positive-stain TEM the gel formed with calcium ions was found to be composed of nanofibers with the same dimensions as those formed by acid-induced self-assembly and by drying on surfaces. This calcium-induced self-assembly may be particularly useful for medical applications where formation of a gel at physiological pH is desired.

## Conclusions

A family of PAs has been demonstrated to self-assemble reversibly into nanofiber networks, which result in the formation of aqueous gels through pH changes. The PA fibers can then be reversibly polymerized to enhance their stability. These two

switchable events controlling the formation of supramolecular structure and polymerization produce a remarkably versatile material. This versatility has been expanded here to include two methods of self-assembly, drying on surfaces and the addition of divalent ions such as calcium. Twelve variants of the PA, with changes in alkyl tail length, the polymerizable region, and the C-terminal peptide sequence all have been shown to self-assemble into a one-dimensional fibrous motif. These molecules demonstrate the ability of the system to tolerate chemi-

cal modification for use in both biological and nonbiological applications.

We thank Bryan Rabatic for assistance with matrix-assisted laser desorption ionization–time of flight MS and the EPIC center at Northwestern University for use of its Hitachi H8100 transmission electron microscope. This work was supported by the Department of Energy (Grant DE-FG02-00ER45810/A001) and the Air Force Office of Scientific Research (Grant F49620-00-1-0283/P01).

- Clark, T. D., Kobayashi, K. & Ghadiri, M. R. (1999) *Chem. Eur. J.* **5**, 782–792.
- Lehn, J. M. (1995) *Supramolecular Chemistry: Concepts and Perspectives* (VCH, Weinheim, Germany).
- Hartgerink, J. D., Clark, T. D. & Ghadiri, M. R. (1998) *Chem. Eur. J.* **4**, 1367–1372.
- Atwood, J. L., Lehn, J. M., Davies, J. E. D., MacNicol, D. D. & Vogtle, F. (1996) *Comprehensive Supramolecular Chemistry* (Pergamon, New York).
- Ghadiri, M. R., Granja, J. R., Milligan, R. A., McRee, D. E. & Khazanovich, N. (1993) *Nature (London)* **366**, 324–327.
- Brunsveld, L., Folmer, B. J. B. & Meijer, E. W. (2000) *MRS Bull.* **25**, 49–53.
- Hirschberg, J. H. K. K., Brunsveld, L., Ramzi, A., Vekemans, J. A. J. M., Sijbesma, R. P. & Meijer, E. W. (2000) *Nature (London)* **407**, 167–170.
- Engelkamp, H., Middelbeek, S. & Nolte, R. J. M. (1999) *Science* **284**, 785–788.
- Isaacs, L., Chin, D. N., Bowden, N., Xia, Y. & Whitesides, G. M. (1999) *Perspect. Supramol. Chem.* **4**, 1–46.
- Whitesides, G. M., Mathias, J. P. & Seto, C. T. (1991) *Science* **254**, 1312–1319.
- MacDonald, J. C. & Whitesides, G. M. (1994) *Chem. Rev.* **94**, 2383–2420.
- Hudson, S. D., Jung, H.-T., Percec, V., Cho, W.-D., Johansson, G., Ungar, G. & Balagurusamy, V. S. K. (1997) *Science* **278**, 449–452.
- Percec, V., Ahn, C.-H., Ungar, G., Yeardley, D. J. P., Moller, M. & Sheiko, S. S. (1998) *Nature (London)* **391**, 161–164.
- Zimmerman, S. C., Zeng, F., Reichert, D. E. C. & Kolotuchin, S. V. (1996) *Science* **271**, 1095–1098.
- Stupp, S. I., Son, S., Lin, H. C. & Li, L. S. (1993) *Science* **259**, 59–63.
- Stupp, S. I., Son, S., Li, L. S., Lin, H. C. & Keser, M. (1995) *J. Am. Chem. Soc.* **117**, 5212–5227.
- Hartgerink, J. D., Beniash, E. & Stupp, S. I. (2001) *Science* **294**, 1684–1688.
- Zubarev, E. R., Pralle, M. U., Sone, E. D. & Stupp, S. I. (2001) *J. Am. Chem. Soc.* **123**, 4105–4106.
- Stupp, S. I., LeBonheur, V., Walker, K., Li, L. S., Huggins, K. E., Keser, M. & Amstutz, A. (1997) *Science* **276**, 384–389.
- Zubarev, E. R., Pralle, M. U., Li, L. & Stupp, S. I. (1999) *Science* **283**, 523–526.
- Tew, G. N., Pralle, M. U. & Stupp, S. I. (2000) *Angew. Chem. Int. Ed.* **39**, 517–521.
- Radzilowski, L. H. & Stupp, S. I. (1994) *Macromolecules* **27**, 7747–7753.
- Won, Y. Y., Davis, H. T. & Bates, F. S. (1999) *Science* **283**, 960–963.
- Pralle, M. U., Urayama, K., Tew, G. N., Neher, D., Wegner, G. & Stupp, S. I. (2000) *Angew. Chem. Int. Ed.* **39**, 1486–1489.
- Israelachvili, J. N., Mitchell, D. J. & Ninham, B. W. (1977) *Biochim. Biophys. Acta* **470**, 185–201.
- Israelachvili, J. N. (1992) *Intermolecular and Surface Forces* (Academic, London).
- Klok, H. A., Langenwalter, J. F. & Lecommandoux, S. (2000) *Macromolecules* **33**, 7819–7826.
- Kogiso, M., Okada, Y., Hanada, T., Yase, K. & Shimizu, T. (2000) *Biochim. Biophys. Acta* **1475**, 346–352.
- Gore, T., Dori, Y., Talmon, Y., Tirrell, M. & Bianco-Peled, H. (2001) *Langmuir* **17**, 5352–5360.
- Hu, J. C., O'Shea, E. K., Kim, P. S. & Sauer, R. T. (1990) *Science* **250**, 1400–1403.
- Berndt, P., Fields, G. B. & Tirrell, M. (1995) *J. Am. Chem. Soc.* **117**, 9515–9522.
- Fields, G. B., Lauer, J. L., Dori, Y., Forns, P., Yu, Y.-C. & Tirrell, M. (1998) *Biopolymers* **47**, 143–151.
- Haverstick, K., Pakalns, T., Yu, Y.-C., McCarthy, J. B., Fields, G. B. & Tirrell, M. (1997) *Polym. Mater. Sci. Eng.* **77**, 584–585.
- Pakalns, T., Haverstick, K. L., Fields, G. B., McCarthy, J. B., Mooradian, D. L. & Tirrell, M. (1999) *Biomaterials* **20**, 2265–2279.
- Yu, Y.-C., Berndt, P., Tirrell, M. & Fields, G. B. (1996) *J. Am. Chem. Soc.* **118**, 12515–12520.
- Yu, Y.-C., Pakalns, T., Dori, Y., McCarthy, J. B., Tirrell, M. & Fields, G. B. (1997) *Methods Enzymol.* **289**, 571–587.
- Yu, Y.-C., Tirrell, M. & Fields, G. B. (1998) *J. Am. Chem. Soc.* **120**, 9979–9987.
- Yu, Y.-C., Roontga, V., Daragan, V. A., Mayo, K. H., Tirrell, M. & Fields, G. B. (1999) *Biochemistry* **38**, 1659–1668.
- Anfinsen, C. B. (1973) *Science* **181**, 223–230.
- Traub, W. & Weiner, S. (1989) *Proc. Natl. Acad. Sci. USA* **86**, 9822–9826.
- Weiner, S. & Wagner, H. D. (1998) *Annu. Rev. Mater. Sci.* **28**, 271–298.
- Harris, J. R. (1991) in *The Practical Approach Series*, eds. Rickwood, D. & Hames, B. D. (Oxford Univ. Press, New York), p. 308.
- Privalov, P. L. & Gills, S. J. (1989) *Pure Appl. Chem.* **61**, 1097–1104.
- Israelachvili, J. N., Mitchell, D. J. & Ninham, B. W. (1977) *Biochim. Biophys. Acta* **470**, 185–201.
- Djabourov, M. (1991) *Polym. Int.* **25**, 135–143.
- Petka, W. A., Hardin, J. L., McGrath, K. P., Wirtz, D. & Tirrell, D. A. (1998) *Science* **281**, 389–392.
- Rodriguez, J. A. & Hrbek, J. (1999) *Acc. Chem. Res.* **32**, 719–728.
- Thompson, H. L., Burbelo, P. D., Yamada, Y., Kleinman, H. K. & Metcalfe, D. D. (1991) *Immunology* **72**, 144–149.
- Tashiro, K., Sephel, G. C., Weeks, B., Sasaki, M., Martin, G. R., Kleinman, H. K. & Yamada, Y. (1989) *J. Biol. Chem.* **264**, 16174–16182.